Verification studies and algorithmic requirements for ALE ideal MHD

Allen Robinson, Greg Weirs,
John Niederhaus, Ed Love

Computational Shock and Multiphysics Department
Sandia National Laboratories

Numerical Methods for Multi-Material Fluids and Structures

Pavia, Italy
September 21-25, 2009

Sandia is a multiprogram laboratory operated by Sandia Corporation, a Lockheed Martin Company, for the United States Department of Energy's National Nuclear Security Administration under contract DE-AC04-94AL85000.

Approved for unlimited release as SAND 2009-5791 C

Basic equations of MHD
less terms for ideal MHD

$$\dot{\rho} + \rho \nabla \cdot \mathbf{v} = 0$$

Balance of mass

$$\rho \dot{\mathbf{v}} = \nabla \cdot \left(\mathbf{T} + \mathbf{T}^M \right) + \mathbf{f}$$

Balance of momentum

$$\rho \dot{e} = \rho s + \mathbf{T} : \mathbf{L} - \nabla \cdot \mathbf{q} + \frac{1}{\sigma} \mathbf{J} \cdot \mathbf{J}$$

Balance of internal energy

$$\overset{*}{\mathrm{B}} = \frac{\partial \mathrm{B}}{\partial t} + \nabla \times (\mathrm{B} \times \mathbf{v}) + \mathbf{v}(\nabla \cdot \mathrm{B}) = -\nabla \times \frac{1}{\mu_0 \sigma} (\nabla \times \mathrm{B})$$

Balance of magnetic flux

$$\frac{d}{dt} \int_{S(t)} \mathrm{B} \cdot d\mathbf{a} + \oint_{\partial S(t)} \mathcal{E} \cdot d\mathbf{x} = 0$$

$$\mathbf{T}^M = \frac{1}{\mu_0} \left(\mathbf{B}\mathbf{B}^T - \frac{1}{2} \mathbf{B}^2 \mathbf{I} \right)$$

Plus thermodynamic stress closure

Maxwell stress tensor

Sandia National Laboratories

ALE MHD ALGORITHM

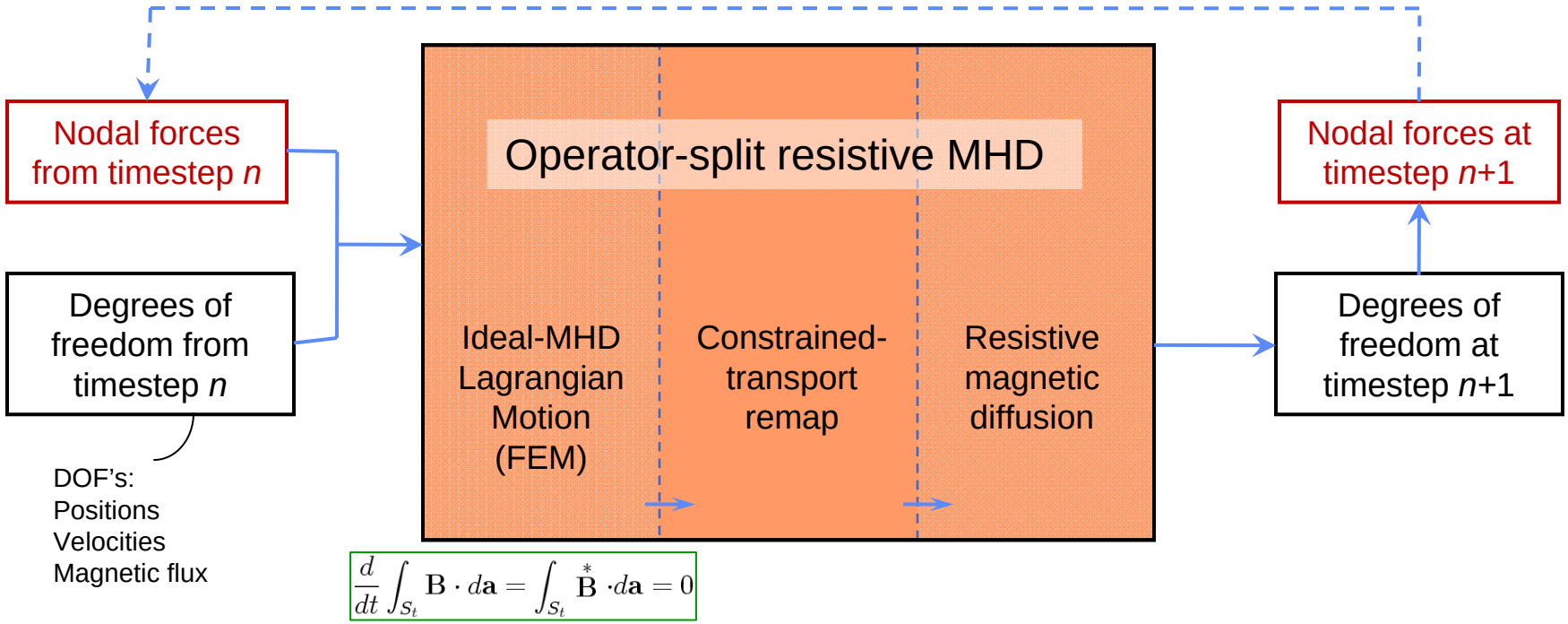

$$\frac{1}{\Delta t}\left[\int_{S(t+\Delta t)} \tilde{\mathbf{B}}^{n+1}\cdot d\mathbf{a}^{n+1} - \int_{S(t)} \mathbf{B}^{n}\cdot d\mathbf{a}^{n}\right] + \frac{1}{\Delta t}\int_{S(t+\Delta t)} (\mathbf{B}^{n+1}-\tilde{\mathbf{B}}^{n+1})\cdot d\mathbf{a}^{n+1} + \oint_{\partial S(t+\Delta t)} \mathcal{E}^{n+1}\cdot d\mathbf{x}^{n+1} = 0$$

Each step preserves a discrete divergence free condition on magnetic flux (involution).

Sandia National Laboratories

Ideal MHD Algorithms

- Integration of equations of motion in Lagrangian frame.
    - Compatible edge/face centering of magnetic quantities
    - Maxwell stress tensor for magnetic forces
    - Central difference time integrator (1st-order time-staggered, unstable in expansion without artificial viscosity)

      OR

      Midpoint predictor-corrector method (2nd-order, stable)
    - Artificial viscosity for shocks based on fast magnetosonic speed.
- Remesh/Remap
    - Constrained transport remap.
    - deBar correction for magnetic energy
- This presentation discusses approaches and results for algorithm verification.

Sandia National Laboratories

Review of Constrained Transport Algorithms

$$\int_V \nabla \cdot \mathbf{B} dV = \oint_S \mathbf{B} \cdot d\mathbf{a} = 0$$

Apply this requirement to the surface of the swept-out volume formed by the remesh motion of an element face:

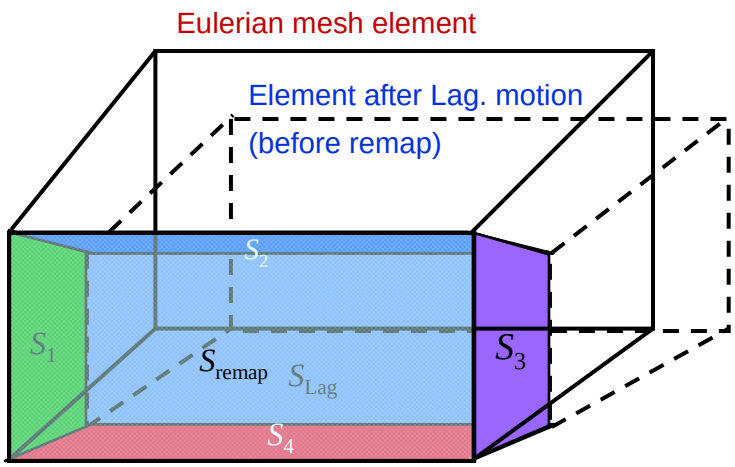

$$\int_{S_{\text{remap}}} \mathbf{B} \cdot d\mathbf{a} + \int_{S_{\text{Lag}}} \mathbf{B} \cdot d\mathbf{a} + \sum_{f=1}^{4} \oint_{\partial S_f} \mathbf{B} \cdot (d\mathbf{x}_f \times d\ell_f) = 0$$

$$\int_{S_{\text{remap}}} \mathbf{B} \cdot d\mathbf{a} = -\int_{S_{\text{Lag}}} \mathbf{B} \cdot d\mathbf{a} + \sum_{f=1}^{4} \oint_{\partial S_f} (d\mathbf{x}_f \times \mathbf{B}) \cdot d\ell_f$$

Flux on remapped surface is the only unknown.

However, accurately evaluating these terms as EDGE quantities requires work

Sandia National Laboratories

Summary of our CT algorithms

- Construct a divergence free, **limited, high-order** representation. This essentially adds cross face flux density contributions.
- Compute the flux integrals associated with each swept edge using the parametric representation of the flux density in the upwind element.
- Take a discrete curl to get updated fluxes (track sign conventions)

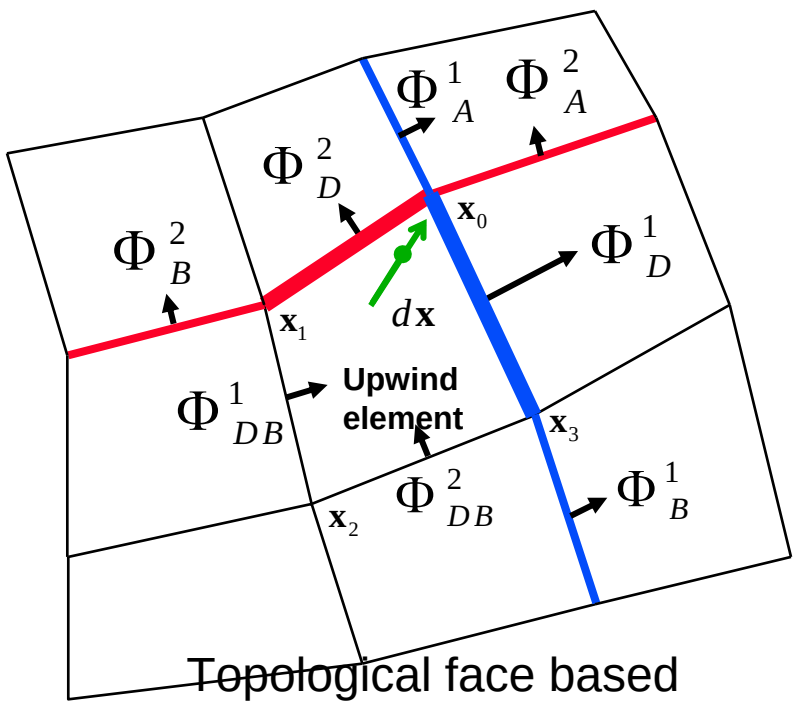

Topological face based reconstruction

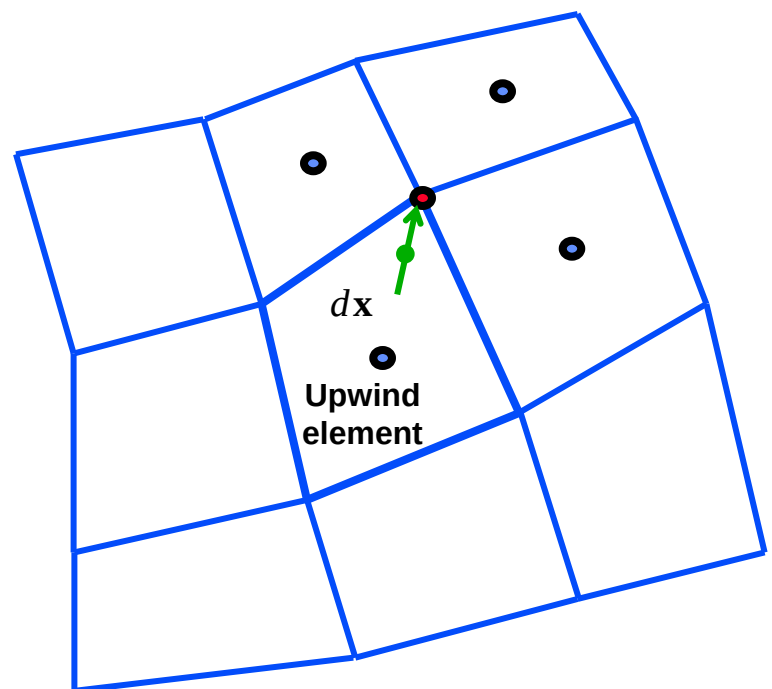

Patch recovery/least squares for nodal B for high order reconstruction

Sandia National Laboratories

2D Face Reconstruction Example

$$\mathbf{x} = (\mathbf{x}_0 + \xi(\mathbf{x}_1 - \mathbf{x}_0)) + \eta[(\mathbf{x}_3 + \xi(\mathbf{x}_2 - \mathbf{x}_3)) - (\mathbf{x}_0 + \xi(\mathbf{x}_1 - \mathbf{x}_0))]$$

$$\mathbf{B} = \sum_f \Phi_f \mathbf{F}_f = \frac{\Phi_D^1(\xi - 1)\frac{\partial \mathbf{x}}{\partial \xi}}{\frac{\partial \mathbf{x}}{\partial \xi} \times \frac{\partial \mathbf{x}}{\partial \eta}} + \frac{-\Phi_{DB}^1 \xi \frac{\partial \mathbf{x}}{\partial \xi}}{\frac{\partial \mathbf{x}}{\partial \xi} \times \frac{\partial \mathbf{x}}{\partial \eta}} + \frac{\Phi_D^2(\eta - 1)\frac{\partial \mathbf{x}}{\partial \eta}}{\frac{\partial \mathbf{x}}{\partial \xi} \times \frac{\partial \mathbf{x}}{\partial \eta}} + \frac{-\Phi_{DB}^2 \eta \frac{\partial \mathbf{x}}{\partial \eta}}{\frac{\partial \mathbf{x}}{\partial \xi} \times \frac{\partial \mathbf{x}}{\partial \eta}}$$

Integrate over flux surface associated with each edge (pointing out of the plane)

$$\int_{S_i} d\mathbf{x} \times \mathbf{B} \approx \delta\eta(\Phi_D^1 + \tfrac{\delta\xi}{2}(\Phi_{DB}^1 - \Phi_D^1)) - \delta\xi(\Phi_D^2 + \tfrac{\delta\eta}{2}(\Phi_{DB}^2 - \Phi_D^2))$$

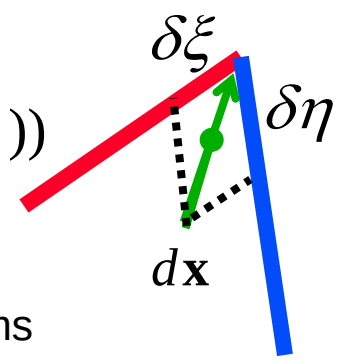

$$\widehat{\Phi}^1(\eta) = \Phi_D^1 + (A_D^1)^2 s^1(\tfrac{1}{2} - \eta)$$

$$\widehat{\Phi}^2(\xi) = \Phi_D^2 + (A_D^2)^2 s^2(\tfrac{1}{2} - \xi)$$

Normal gradient terms

Limited high order terms dependent on the cross face coordinate replace the original low order flux in the edge integrals.

Sandia National Laboratories

3D Patch Recovery

$$\begin{aligned}\mathbf{B}(\xi_1,\xi_2,\xi_3) &= \Phi_1^+(\xi_2,\xi_3)\mathbf{W}_1^+ + \Phi_1^-(\xi_2,\xi_3)\mathbf{W}_1^- + \\ &\quad \Phi_2^+(\xi_3,\xi_1)\mathbf{W}_2^+ + \Phi_2^-(\xi_3,\xi_1)\mathbf{W}_2^- + \\ &\quad \Phi_3^+(\xi_1,\xi_2)\mathbf{W}_3^+ + \Phi_3^-(\xi_1,\xi_2)\mathbf{W}_3^-\end{aligned}$$

$$\Phi_i^+(\xi_2,\xi_3) = \Phi_i^+ + s_{i2}^+\xi_2 + s_{i3}^+\xi_3$$

Use least square representation at nodes to compute s values at nodes

$$\begin{aligned}4\det J_F(p)\quad \mathbf{B}(p) = \quad & \Phi_1^+(1,0)\mathbf{V}_1(p) + \\ & \Phi_2^+(0,1)\mathbf{V}_2(p) + \\ & (\Phi_3^+(1,1) + \Phi_3^-(1,1))\mathbf{V}_3(p)\end{aligned}$$

$$\begin{aligned}4\mathbf{B}(p)\cdot(\mathbf{V}_2(p)\times\mathbf{V}_3(p)) &= \Phi_1^+(1,0) \\ 4\mathbf{B}(p)\cdot(\mathbf{V}_3(p)\times\mathbf{V}_1(p)) &= \Phi_2^+(0,1)\end{aligned}$$

Limit (harmonic limiting)

$$\begin{aligned}s_{12}^+ &= 2s_{12}^{++}s_{12}^{+-}/(s_{12}^{++}+s_{12}^{+-}),\ \text{if} s_{12}^{++}s_{12}^{+-} > 0 \\ s_{12}^+ &= 0,\ \text{otherwise}\end{aligned}$$

Edge integration

$$\hat{\xi}_i = \frac{\delta\xi_i}{2} + \xi^{ec}$$

$$\begin{aligned}\int_S \mathbf{B}\cdot d\mathbf{a} &\approx \frac{1}{4}(-\Phi_2^+(\hat{\xi}_3,\hat{\xi}_1)(1+\hat{\xi}_2) - \Phi_2^-(\hat{\xi}_3,\hat{\xi}_1)(1-\hat{\xi}_2))\delta\xi_1 \\ &+ \frac{1}{4}(\Phi_1^+(\hat{\xi}_2,\hat{\xi}_3)(1+\hat{\xi}_1) + \Phi_1^-(\hat{\xi}_2,\hat{\xi}_3)(1-\hat{\xi}_1))\delta\xi_2\end{aligned}$$

Sandia National Laboratories

Symmetry Verification

Verification means that we check our solution by comparing against some other computational method.

We have found that simple symmetry requirements are excellent first checks.

For example, CT does not conserve energy but you can still verify that the energy loss is the same for solutions which should be invariant independent of flow direction.

The properties can be checked completely automatically. The testing framework should support runs of multiple tests with varying parameters.

The verification work does not count until the test is encapsulated and running in the automated testing framework. That is, the test must leave the developer's hands and end up in the team's repository and process.

It is much better to implement a simple verification check than no verification!

Sandia National Laboratories

Order Verification for ALE MHD

Order verification means we examine convergence rates for wave propagation problems whose solution is available.

1. Smooth: Alfvén waves

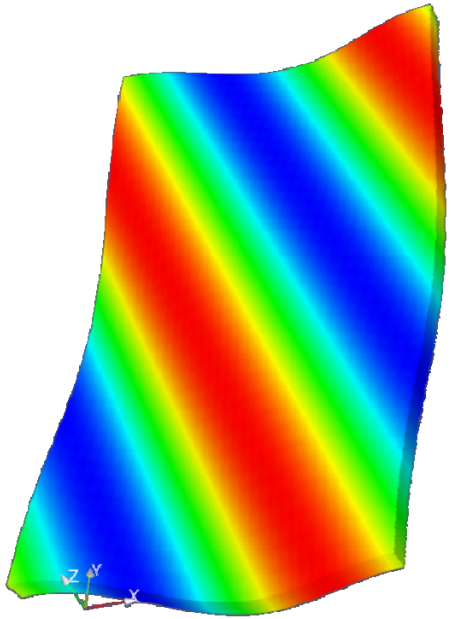

Circularly polarized Alfvén wave.

2. Discontinuous: MHD shocks (self steepening)

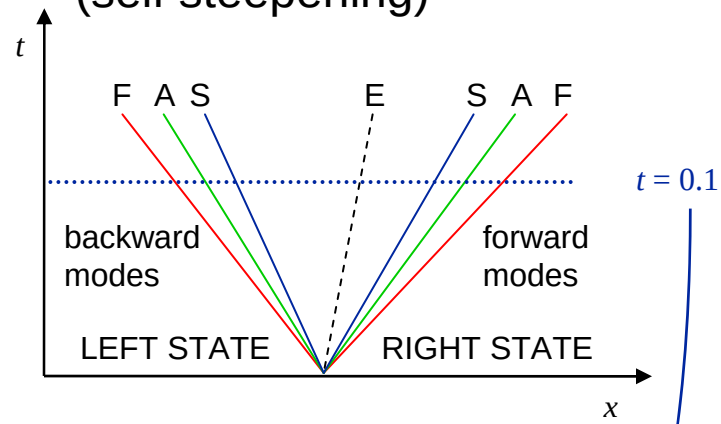

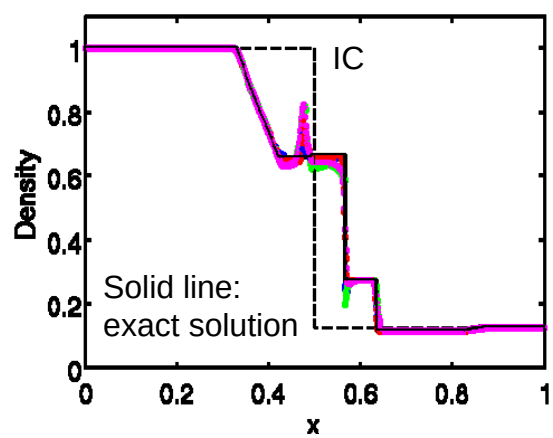

Problem 5(a), Ryu & Jones, *Ap. J.*, 1995.

Sandia National Laboratories

Circularly polarized Alfvén wave problem

Alfvén wave: a non-compressive, isentropic, transverse disturbance in the velocity and **B** field only, propagating along lines of magnetic force with a velocity

$$v_A = \sqrt{\frac{B_{\parallel}^2}{\mu\rho}}$$

Following Toth (JCP, 2000), a continuous train of circularly polarized Alfvén waves is initialized in ALEGRA as:

$$B_z(x,y) = v_z(x,y) = a\cos\theta(x,y)$$
$$B_\perp(x,y) = v_\perp(x,y) = a\sin\theta(x,y)$$
$$\theta(x,y) = 2\pi(x\cos\alpha + y\sin\alpha)$$

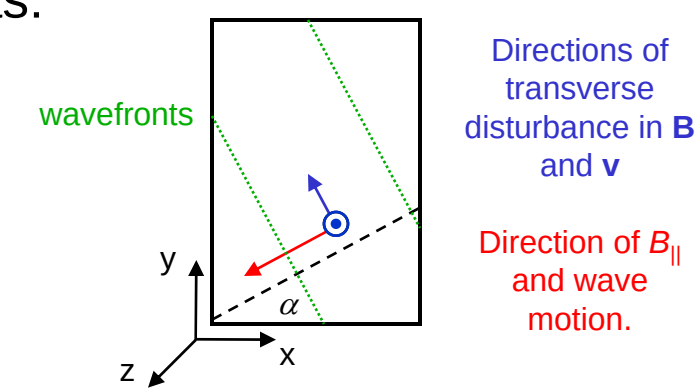

With α = 30°, $v_{\parallel}$ = 0, $B_{\parallel}$ = 1, and ρ = 1, the wave train translates at 30° to the *x*-axis, with unit wavelength and period $\tau = 2\pi/\omega = 2\pi k / v_A = 1$.

→ Exact solution is identical to IC for integer time *t*.

Verification Approach

Code Verification

- reference solution is exact
- ideal for testing algorithms and their implementations

- code verification in space: fixed CFL, various mesh resolutions
- the initial solution is the reference at periodic times

Solution Verification

- solution is extrapolated from simulations at different resolutions
- usually used for error estimation in production calculations

- solution verification in time: one mesh, various (constant) Δt's
- reference solution generated from the two solutions with the smallest time steps

- Artificial Viscosity is turned off for this shock-free problem
- All remaps are CT remaps, but different limiters are used

Sandia National Laboratories

Code Verification

Spatially 2nd-Order Accurate

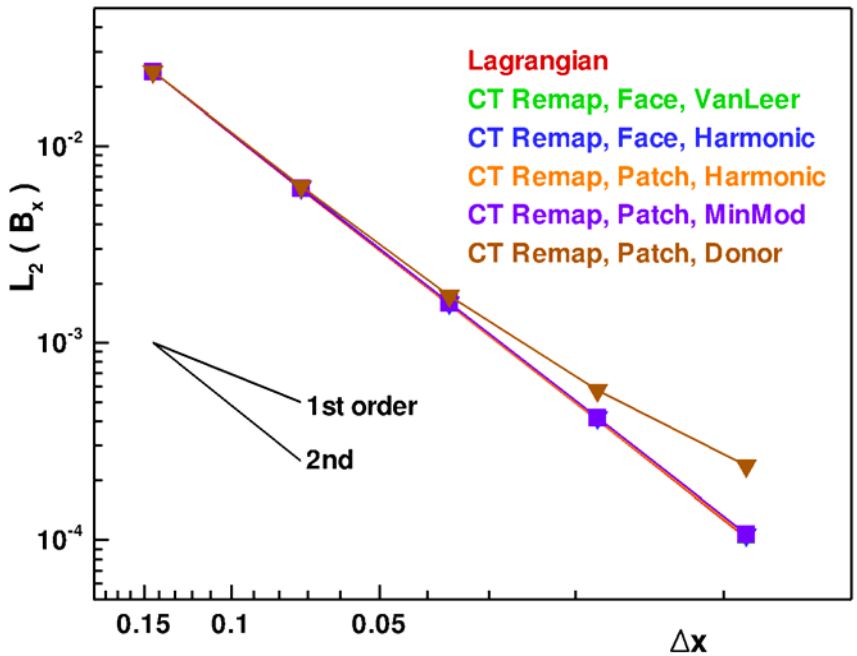

- Predictor-Corrector time integrator
- L_2 norm of B_x at t=1.0
- Results for other components and velocity are the same
- Convergence rates degrade on coarser meshes for t=2.0

Nominally 2nd-order, except for Donor-cell limiter (as expected)

Sandia National Laboratories

Solution Verification

Spatial Error Dominates Temporal Error

First we tried code verification; no convergence as $\Delta t \to 0$.

Hunch: temporal error is in the noise compared to spatial error

How to isolate the temporal error? Solution verification.

- All the simulations are done on the same mesh.
- Assume the spatial and temporal errors are independent.
- Then the extrapolated solution has the same spatial error as each of the other solutions
- So the differences between simulations and the extrapolated solution are due to temporal error only.

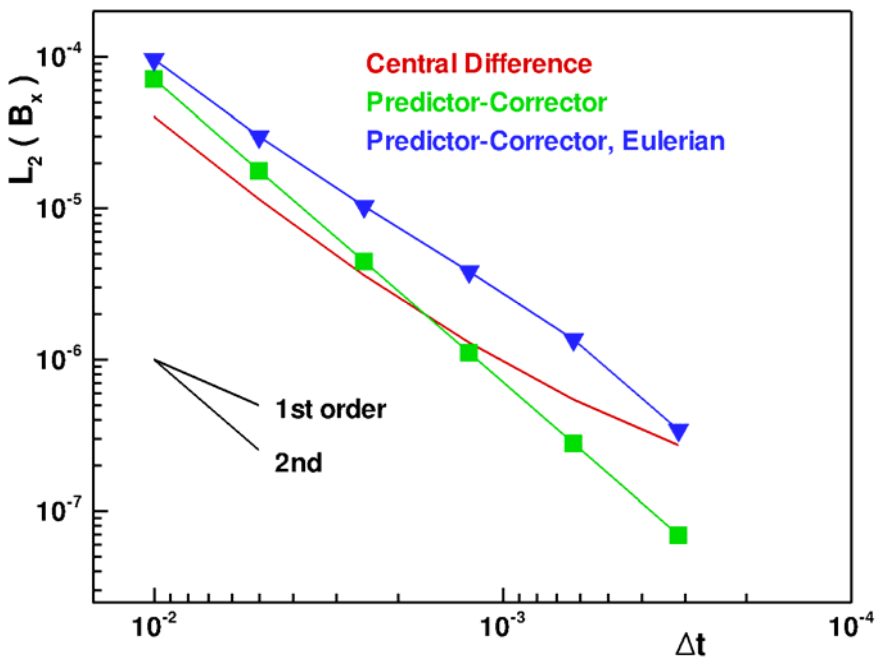

Predictor-Corrector: 2nd-order temporal convergence

Central Difference: 1st-order

Eulerian simulations show reduced order of accuracy in time

Sandia National Laboratories

Does Temporal Accuracy Matter?

For ALEGRA, Stability Motivates Predictor-Corrector

- Stability is driving the adoption of the predictor-corrector time integrator
- Demonstrating 2nd-order accuracy shows correct implementation

Lineout at y=0.8, t=1.0
CFL = 0.95

Central Difference:
growing oscillations (color)

Predictor-Corrector:
no oscillations

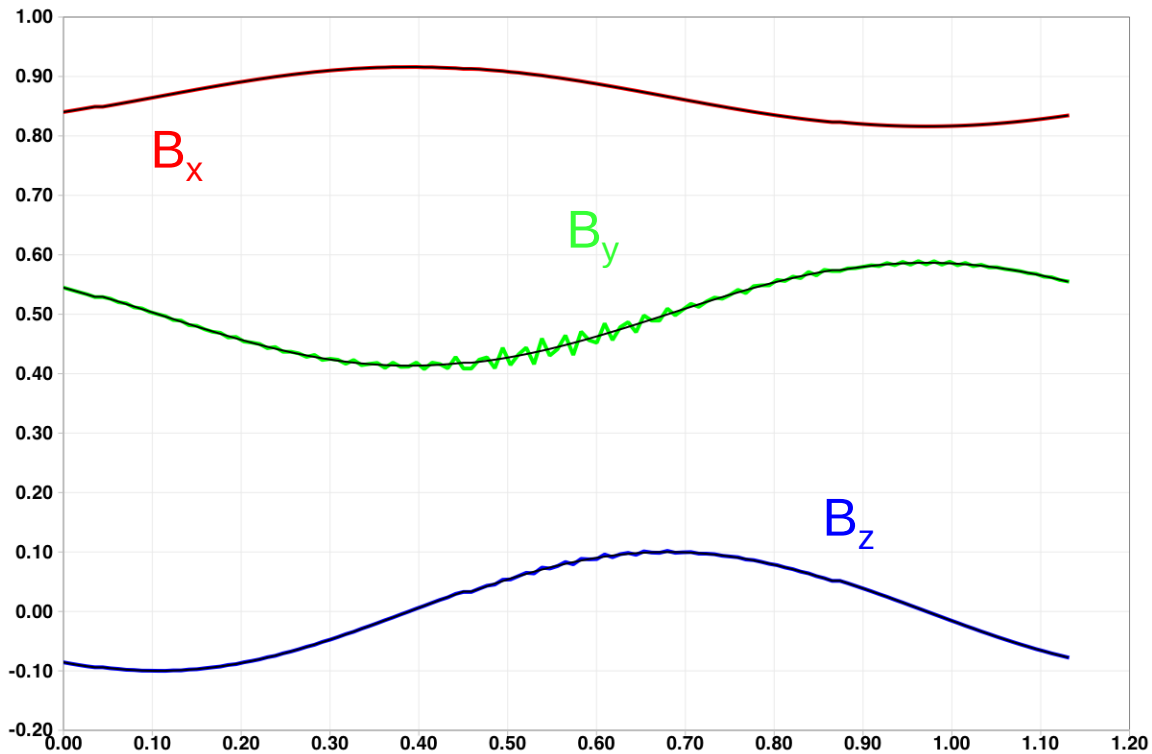

Sandia National Laboratories

Magnetized Noh problem

As a test of MHD shock treatment, we also consider problems involving nonlinear, self-steepening MHD waves:

1. Magnetized Noh problem: supersonic stagnation flow

Initial condition:

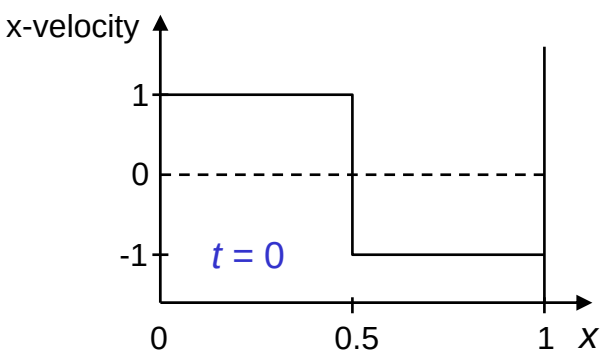

$$\mathbf{B} = \frac{1}{2}(\hat{x} + \hat{y})$$

$\rho = 1.0$
$p = 10^{-6}$

Time-space plot:

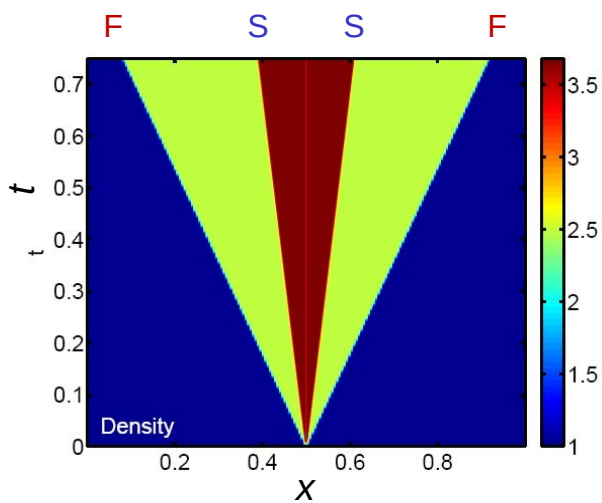

- Standard test problem in shock hydrodynamics*
- Ideal-gas EOS
- Oblique, transverse **B** field added
- Ideal MHD
- Very strong MHD shocks
- Exact solution can be computed using ideal-MHD Riemann solver

*Noh, *J. Comp. Phys.*, 1979

DeBar correction

ALEGRA uses a modern implementation of DeBar's correction for the kinetic energy loss arising in elements near shocks due to remap:

conservatively remapped KE

actual remapped KE

$$\Delta E_k = \frac{1}{N}\sum_{n=1}^{N}\frac{1}{2}\mathcal{R}[m](\mathcal{R}[\mathbf{v}_n]\cdot\mathcal{R}[\mathbf{v}_n]) - \mathcal{R}\left[\frac{1}{N}\sum_{n=1}^{N}\frac{1}{2}m(\mathbf{v}_n\cdot\mathbf{v}_n)\right]$$

$$E_i^{\mathrm{DeBar}} = E_i + \Delta E_k$$

$\mathcal{R}[.]$ = remap operator

m = mass associated with element

$\mathbf{v}_n$ = nodal velocity

The traditional form of the DeBar correction maintains full conservation of energy in remap for pure hydrodynamics.

Optional limiters are included in the implementation:

- Restrict to shocks only, using value of Q/P
- Limit magnitude of correction in the case of cooling

Sandia National Laboratories

DeBar correction

DeBar's correction is extended in ALEGRA to include magnetic energy losses arising in the solution due to remap:

$$\Delta E_m = \frac{1}{2\mu_0} \sum_{q=1}^{Q} \left[w_q \left(\sum_{f=1}^{F} \mathcal{R}[\Phi_f] \mathbf{W}_f(x_q) \right)^2 \right] - \mathcal{R}[E_m]$$

conservatively remapped ME

actual remapped ME

$$E_i^{\mathrm{DeBar}} = E_i + \Delta E_k + \Delta E_m$$

w_q = element shape functions

$\mathbf{W}_f$ = vector face shape functions

Φ_f = magnetic flux on face *f*

With the magnetic DeBar correction implemented, full conservation of total energy and its components is maintained in remap by ALEGRA.

Same limiters apply for hydrodynamic and magnetic DeBar correction.

Sandia National Laboratories

Magnetic Noh Test Results

Debar Corrections Required for Convergence

Code Verification in space:

- constant CFL=0.95
- Central difference time integrator
- 16, 32, 64, 128, 256, 512 elements
- Results shown at t=0.75

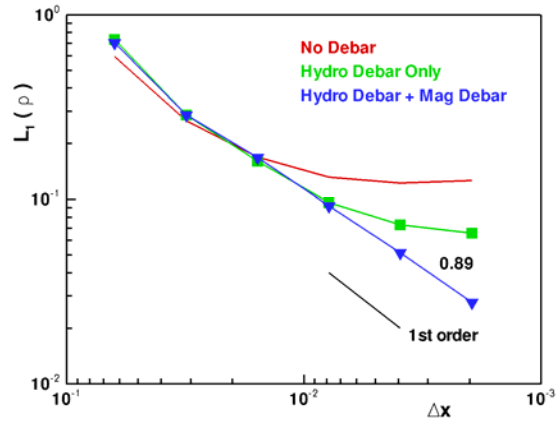

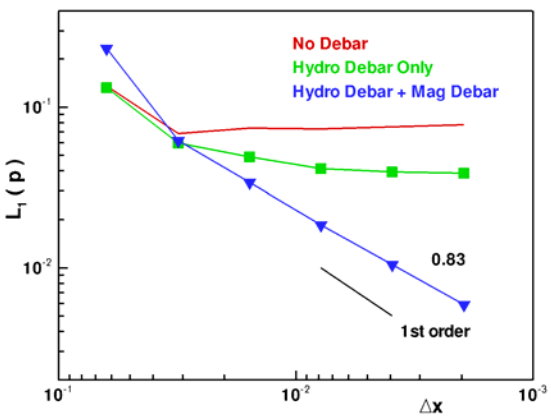

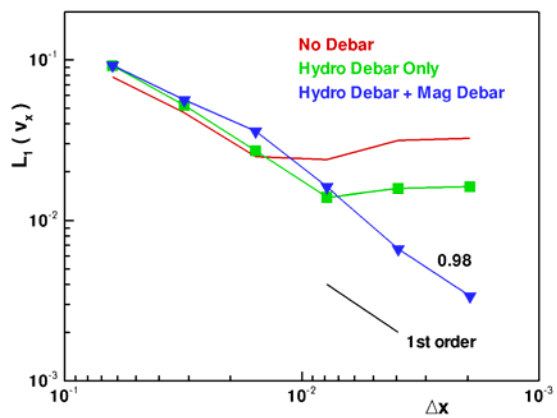

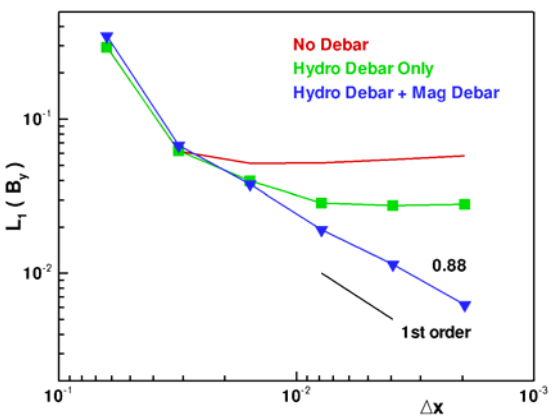

Sandia National Laboratories

Magnetized Noh Shock Profiles

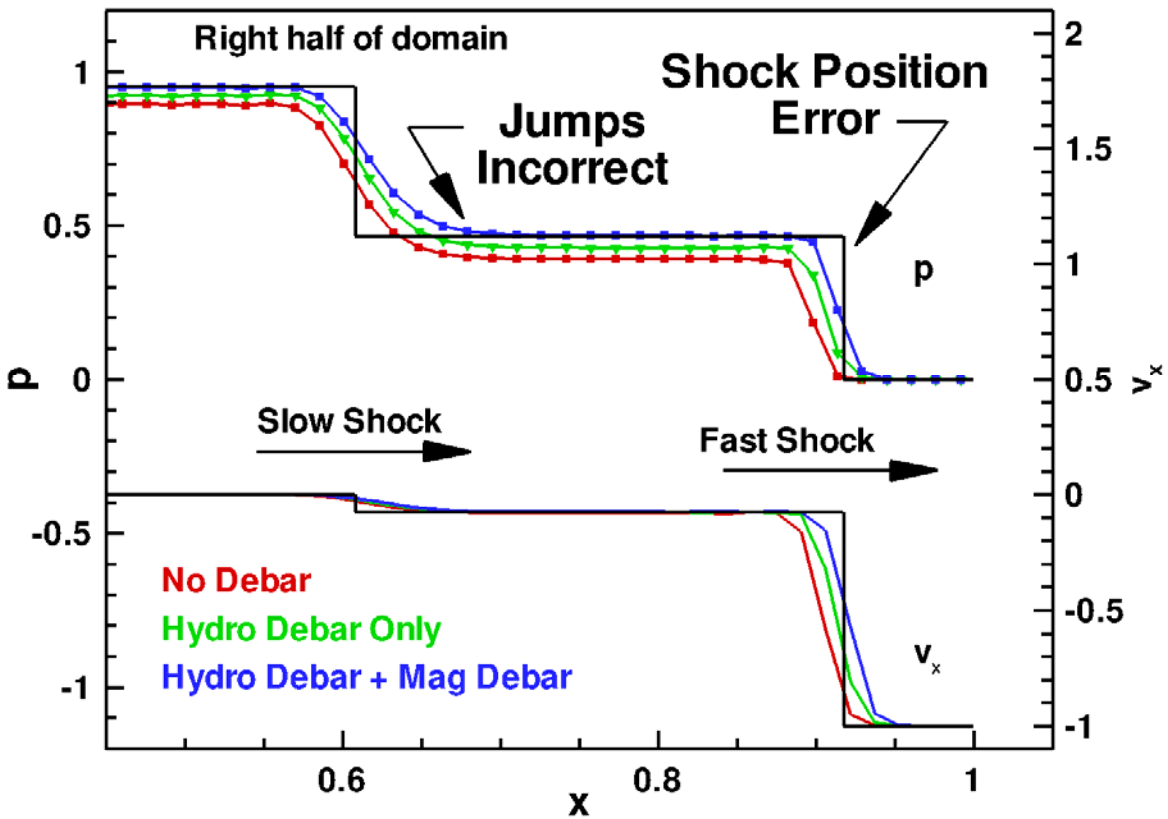

- Shock speeds mispredicted
- Wrong post-shock state

Sandia National Laboratories

Magnetized Woodward-Colella problem

A second problem provides a more stringent test of shock capability, though without the possibility of rigorous code verification:

2. Magnetized Woodward-Colella problem: interacting blast waves

Initial condition:

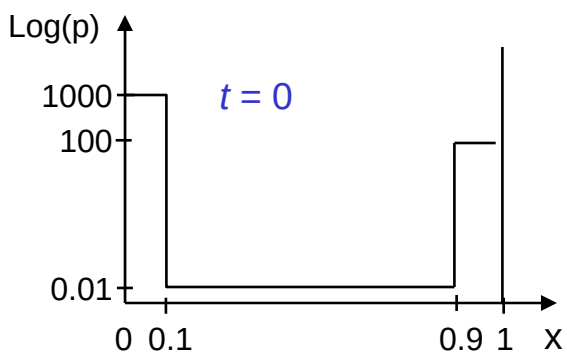

$\mathbf{B} = 15(\hat{x} + \hat{y})$

$\rho = 1.0$
$\boldsymbol{v} = 0.0$

Time-space plot:

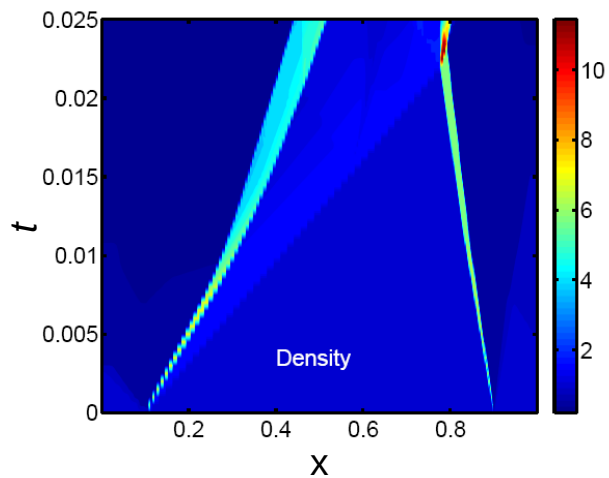

- Standard test problem in shock hydrodynamics*
- Ideal-gas EOS
- Oblique, transverse **B** field added
- Ideal MHD
- Very strong MHD shocks
- No exact solution available; reference solution can be computed using ideal-MHD Godunov method (Athena)**

*Woodward and Colella, *J. Comp. Phys.*, 1984
**Gardiner and Stone, *J.Comp. Phys.*, 2005

Results with energy conservation

Acceptable convergence observed only with full energy conservation via Debar:

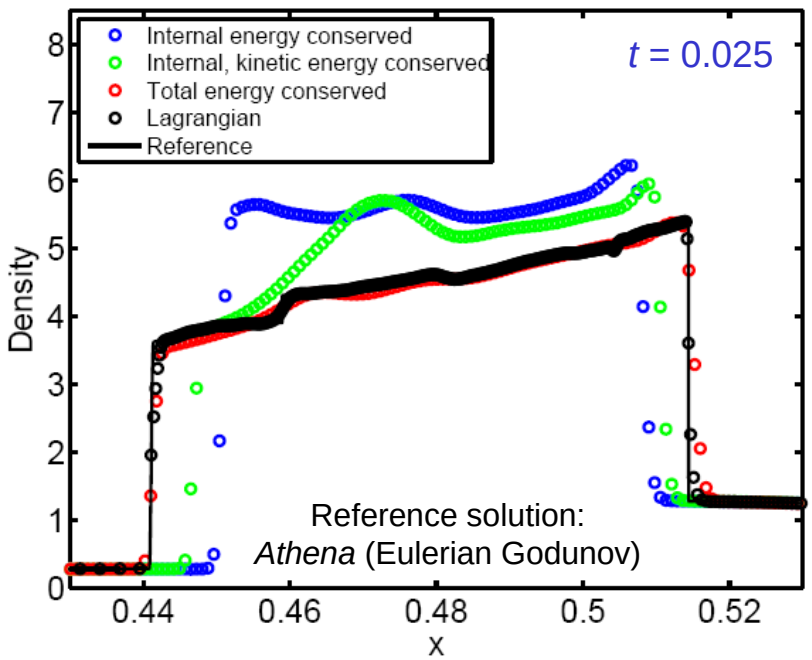

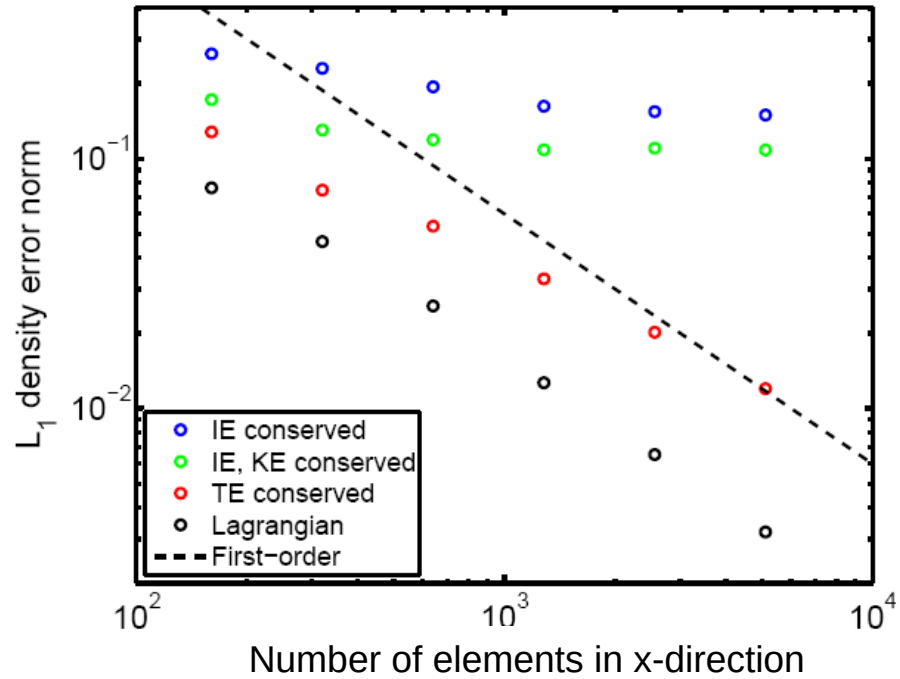

	Grid sizes	160/320	320/640	640/1280	1280/2560	2560/5120
No DeBar →	IE conserved	0.194	0.245	0.258	0.071	0.047
KE DeBar →	IE,KE conserved	0.403	0.129	0.135	-0.023	0.024
Full DeBar →	TE conserved	0.773	0.480	0.700	0.709	0.750
	Lagrangian	0.717	0.855	1.022	0.954	1.031

Sandia National Laboratories

Issues

- The DeBar correction, in its current implementation, introduces robustness issues.
  - Adjustment to internal energy can have either sign; thus, it can introduce negative temperatures in some cases
  - The correction also introduces anomalous behavior at contacts in some cases.
  - Limiters can be applied to address these issues, but then energy is again not fully conserved.
  - Energy redistribution should have a more consistent node weighting
- Artificial viscosity for MHD shock (7 modes, with transverse modes) should be improved.

Sandia National Laboratories

Summary

- Application of a formal verification methodology has been of significant use in gaining confidence in ideal MHD algorithms and implementations. Both simple and more extensive order verification methods are highly useful.
    - Symmetry tests
    - Order verification
- All verification tests must be implemented in a team owned test harness which is run on a regular basis.
- Verification suite clearly points out fruitful avenues for future research and provides the basis for future success.
    - deBar robustness
    - Artificial viscosity for MHD shock

Sandia National Laboratories